ELSEVIER

FUEL

Conversion of natural gas to liquids via acetylene as an intermediate ☆

R.P. Anderson[a,*], J.R. Fincke[a], C.E. Taylor[b,1]

[a]Idaho National Engineering and Environmental Laboratory (INEEL), P.O. Box 1625, Idaho Falls, ID 84315-2110, USA
[b]National Energy Technology Laboratory (NETL), P.O. Box 10940, Pittsburgh, PA 15236, USA

Received 12 December 2000; revised 10 January 2001; accepted 10 January 2001; available online 4 December 2001

Abstract

This paper describes an experimental investigation of the conversion of natural gas to liquid transportation fuels through acetylene as an intermediate. The first step is the direct thermal conversion of methane to acetylene utilizing a thermal plasma heat source to dissociate the methane. The dissociation products react to form a mixture of acetylene and hydrogen. Significant improvements over the prior art were observed; these improvements may be attributed to an improved methane injection configuration and minimization of radial temperature gradients. Conversion efficiencies (percent methane converted) approached 100% and acetylene yields in the 90–95% range with 2–4% solid carbon production were obtained. A variety of methods were examined for the second step, the conversion of acetylene to liquid products. The most promising technology was the reaction of acetylene with hydrogen over a shape-selective zeolite to form C_3–C_5 + aliphatics.

Keywords: Gas-to-liquids; Methane conversion; Acetylene

1. Introduction

1.1. Gas-to-liquids

Large quantities of natural gas exist in many remote parts of the world where there is no economical means of transporting it to end use markets for conventional use. The objective of the work reported in this paper is to develop a process whereby the natural gas that is located in a remote location (e.g. the North Slope of Alaska) can be converted to a liquid that can be transported to market utilizing existing infrastructure. Currently, there are two broad gas-marketing schemes proposed for commercializing natural gas on the North Slope. One is a gas pipeline/liquefied natural gas scenario; the other is a gas-to-liquids option that chemically converts the natural gas to a stable liquid syncrude in a North Slope plant, eliminating the need for an additional pipeline from the North Slope to a southern Alaska port [1]. The conventional gas-to-liquids approach involves synthesis gas generation followed by Fischer–Tropsch synthesis. The Alaska Department of Revenue compiled a brief comparison of six variations of this technology: Basic Fischer–Tropsch technology, Sasol's Fischer–Tropsch technology, Exxon's AGC-21, BP's compact steam reformer, Syntroleum's air blown autothermal technology, and a Fischer–Tropsch process using DOE's ceramic membrane [1]. In the research described in this paper, an alternative gas-to-liquids approach is investigated. This involves the thermal conversion of natural gas to acetylene followed by catalytic conversion of acetylene to liquid products.

1.2. Acetylene from natural gas

Acetylene has been produced commercially from methane since the 1940s. However, the efficiency of the conversion and acetylene yields had not been optimized. The objective of this project was to determine if the modest methane conversion efficiencies, acetylene yields and selectivities, and specific energy requirements previously observed could be improved upon.

Chemische Werke Hüels has been using an electric arc process to produce acetylene since the 1940s [2]. The original Hüels plant used the low-boiling components of the motor fuel industry as raw material; however, a wide range of hydrocarbons including natural gas was shown to be suitable as process feedstocks. The plasma gas consists of methane and/or hydrogen. Heavier hydrocarbons are injected downstream of the discharge. The residence time in the discharge and reactor section is on the order of

* Corresponding author. Tel.: +1-208-526-1623; fax: +1-208-526-9822.
E-mail addresses: anderp@inel.gov (R.P. Anderson), charles.taylor@netl.doe.gov (C.E. Taylor).
[1] Tel.: +1-412-386-6058; fax: +1-412-386-4806.
☆ Published first on the web via Fuelfirst.com-http://www.fuelfirst.com

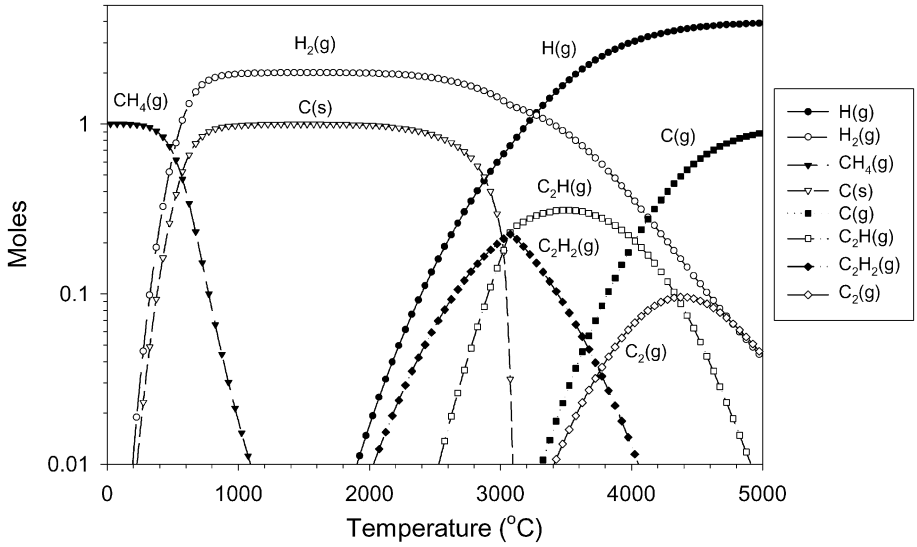

Fig. 1. Simplified equilibrium diagram for methane.

milliseconds (ms). Immediately downstream of the reactor section the gas is abruptly cooled by liquid water spray injection. The dissociation of all hydrocarbons into carbon and hydrogen begins at relatively low temperatures. For example, the dissociation of methane begins at around 500 °C and is completed by 1000 °C. If the process is strictly in equilibrium, the thermodynamically preferred products between about 1000 and 2500 °C are solid carbon and molecular hydrogen (H_2) [3], Fig. 1. As the temperature increases, hydrogen dissociates ($T > 2500$ °C) and acetylene forms, reaching a maximum concentration at $T \cong 3000$ °C. The equilibrium formation of acetylene is characterized by the requirement of very high temperatures, around 3000 °C. Assuming that upon cooling the C_2H radical combines with either atomic or molecular hydrogen to produce acetylene, the maximum theoretical yield, defined as the amount of carbon contained in the acetylene formed divided by the amount of carbon in the methane feedstock, is approximately 91%. Because the formation of acetylene from methane is strongly endothermic, relatively large amounts of energy are required per unit mass of acetylene formed.

In practice, however, the rate of formation of unsaturated hydrocarbons, acetylene and ethylene, is much faster than the complete decomposition reaction and the subsequent formation of solid carbon soot. It is known that the formation of polycyclic aromatic hydrocarbons is a major nucleation mechanism for soot [4]. Benzene rings and higher aromatics are thought to be formed from acetylene. The polycyclic aromatic hydrocarbons increase in molecular weight by acetylene addition and become hydrogen deficient by hydrogen abstraction leading to the formation of primary soot particles. These primary soot particles continue to grow via the decomposition of acetylene on their surfaces. Hence the formation of acetylene precedes decomposition into soot and hydrogen. If the product stream is rapidly cooled or quenched to temperatures where the products are stable before soot has time to nucleate and grow, the desired composition is frozen in. A second, modified equilibrium composition diagram [3] for the methane (CH_4) system is shown in Fig. 2. In this calculation, the solid phase of carbon is not considered as a possible product. The result is the formation of acetylene with a maximum theoretical yield of 98.5% at a temperature of around 1875 °C. The Hüels process operates in this lower temperature regime.

Even at the reduced temperature of 1875 vs. 3000 °C, the process cannot readily be realized by heat transmission through vessel walls because of materials limitations. In addition, to avoid the formation of solid carbon soot, heating should be as rapid as possible followed immediately by a rapid quench. Arc heating accomplishes the rapid heating, and a water spray quench is used in the Hüels process to rapidly cool the product stream. The quench rates obtained in the Hüels process are reportedly 700 °C in approximately 1 ms. We will regard the Hüels process as the benchmark to be compared against. These comparisons will be made quantitative through the calculation of various yield, conversion efficiency (CE), and energy consumption metrics. Only feedstocks containing predominately methane (natural gas) will be considered.

Relevant results from the available literature on acetylene derived from hydrocarbons by the electric arc process are tabulated in Table 1. CE is defined as the percent of feedstock (methane or natural gas) which is converted to some product; acetylene yield is defined as the percentage of carbon in the feedstock which ends up as acetylene, and the specific energy requirement is the electrical consumption in kilowatt hours (kW h) per kilogram (kg) of acetylene produced. The original Hüels plant used the low boiling components of the motor fuel industry as raw material, although feedstocks ranging from natural gas [2] to coal

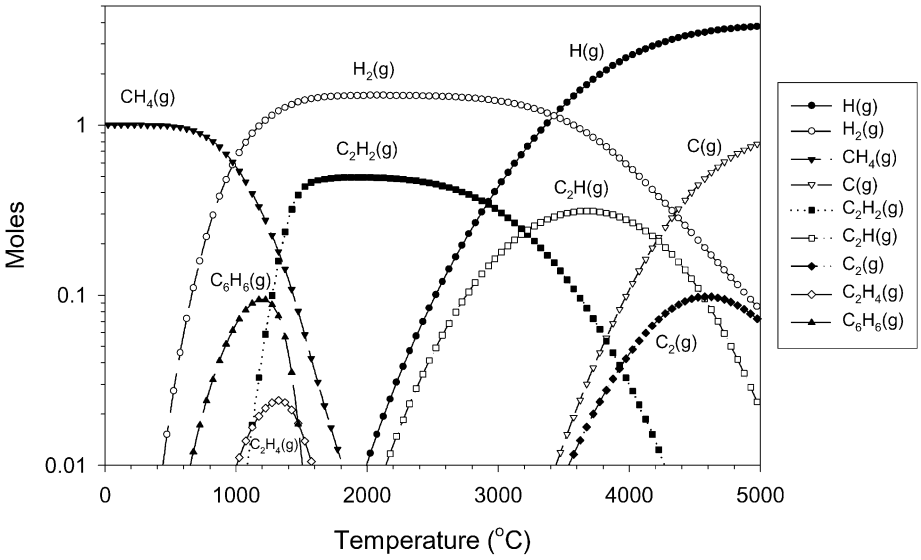

Fig. 2. Simplified equilibrium diagram for methane where the solid phase of carbon is not included as a species.

[5,6] have been examined. A similar process with reactors of similar size (9 MW) was built by DuPont and operated between 1963 and 1968 supplying acetylene produced from liquid hydrocarbon sources to a neoprene plant [7]. In the DuPont process, the arc was magnetically rotated, while in the original Hüels process, the arc is 'swirl stabilized' by tangential injection of gases. In the DuPont process all feedstock, diluted with hydrogen, passed through the arc column; in the Hüels process, a fraction of the reactants are injected downstream of the arc.

The Hüels and DuPont processes represent the only industrial scale demonstrations of the conversion of methane to acetylene by the plasma arc process. When operated on methane, both the reported yield and specific energy requirement of the DuPont process appear to be somewhat improved over that of the Hüels process, 70 vs. 50% for yield and specific energy requirement of 8.8 vs. 12.1 kW h kg^{-1} C_2H_2. Because the reported yields for the DuPont process for hydrocarbon feedstock up to C_{10} are reported to be in the range of 65–75 vs. 50% for the Hüels process, the data suggest that there is, in fact, a fundamental difference between the Hüels and DuPont processes. The amount of hydrogen introduced as plasma gas may have an effect on the reported results as may pressure and magnetic arc rotation. Lower pressure and higher hydrogen concentrations may inhibit soot and the formation of other hydrocarbons while magnetic arc rotation may lead to a better 'stirred' reactor.

In addition to the Hüels and DuPont work, there have been a number of laboratory scale investigations generally conducted at less than 10 kW power levels. These investigations have generally utilized direct current plasma jets. The electrical discharge heats argon, hydrogen or a mixture of the two. In one case, a radio frequency plasma is used and the plasma gas is helium. Methane (or natural gas) is injected downstream of the discharge and mixes with the hot gas jet. The predominant method of quenching is wall heat transfer to cooling water. Reported conversion efficiencies are generally in excess of 90% while acetylene yields range from 76 to 86%. The yield of other hydrocarbons or solid carbon soot is generally not reported in the literature cited. The measured specific energy requirement ranges from a high of 88 to a low of 9 kW h kg^{-1} C_2H_2. This value should be compared to a theoretical value of 7.9 kW h kg^{-1} C_2H_2 for a product stream at 2000 °C, 100% acetylene yield and 100% conversion and thermal efficiency. Because direct current plasma devices, particularly, small-scale ones with low volume to heat loss area ratio, are rarely better than 70–85% thermally efficient, that is, 70–85% of the discharge power is deposited in the gas stream and the rest is lost to cooling water, any reported specific energy requirement less than about 9.5 kW h kg^{-1} C_2H_2 should be critically regarded. As discharge and plasma reactors are scaled to larger sizes the system thermal efficiency can often be improved.

The fundamental question that is addressed in this study is whether the modest methane conversion efficiencies, acetylene yields and selectivities and specific energy requirements observed in the original Hüels process can be substantially improved upon. Central to this issue is the identification of mechanisms that are responsible for lowering the observed CE and yield values and investigation of possible solutions. The two immediately apparent possibilities are as follows: (1) steep radial temperature gradients and poor mixing in the reactor, and (2) a quenching process that is not rapid enough to freeze the composition of the product stream.

Temperature gradients and poor mixing lead to a non-uniform distribution of temperatures in the reactor. The composition of the product stream is a function of kinetics and the temperature non-uniformities, which can lead to significant variations in product stream composition. If the

Table 1
Summary of prior results on the plasma conversion of natural gas to acetylene

Reference	Year	Process	Reactor size	Feedstock	Plasma gas	Quench method	Conversion efficiency (%)	Maximum acetylene yield (%)	Normalized acetylene yield (%)	Soot yield (%)	Minimum specific energy requirement for C_2H_2 (kW h kg^{-1})
Leutner and Stokes [22]	1961	DC plasma jet	6.8 kW	CH_4	Ar	Wall heat transfer	92.9	80.1	86.2	5.7	72.5
Gladisch [2]	1962	Hüels DC arc	8 MW	Natural gas	CH_4	Water spray	70.5	51.4	72.9	2.7	12.1
Anderson and Case [23]	1962	DC plasma jet	< 10 kW	CH_4	H_2	Water spray	> 90	76	88	Not analyzed	9.16
Holmes [7]	1969	DuPont DC arc	9 MW	CH_4	H_2	Not reported	Not reported	70		Not reported	8.8
Ibberson and Sen [24]	1976	DC plasma jet	< 10 kW	CH_4	Ar	Wall heat transfer	> 90	82	91	Not analyzed	9.0
Plotczyk [25]	1983	DC plasma jet	10–40 kW	CH_4	H_2	Wall heat transfer	95	80	84	Not analyzed	15.5
Kovener [26]	1983	RF plasma	4 kW	CH_4 and natural gas	He	Wall heat transfer	Not reported	Not reported	–	Not reported	88
Plotczyk [27]	1985	DC plasma jet	4–16 kW	CH_4	Ar	Wall heat transfer	> 90	86	95	Not reported	23.9

quench process is too slow or delayed, the acetylene produced can thermally decompose to solid carbon soot [4,8] or may further react to form benzene and heavier hydrocarbons. These issues are experimentally addressed in a nominally 75 kW laboratory reactor system. The issue of non-uniform temperatures is examined using a carbon lined 'hot wall' reactor configuration, which minimizes the radial temperature gradients and heat loss from the reactor section. The issue of poor mixing is addressed through the use of a confined channel injector design, which has been shown to provide good mixing of reactants into a plasma stream [9]. The effect of quench rate is addressed by the incorporation of a supersonic quench nozzle into the test apparatus, just downstream of the reactor section [10]. In the supersonic nozzle, the hot gases in the reactor section are rapidly expanded to a lower pressure converting thermal energy to kinetic energy and the mixture is rapidly cooled. Quench rates of 10^7–10^8 °C s^{-1} or two to three orders of magnitude greater than those reported in the original Hüels process are achievable.

1.3. Acetylene to liquids

There is extensive literature on the chemistry of acetylene predating the 1930s [11]. The early chemistry of acetylene involved primarily polymerization reactions. These reactions were conducted by heating of the acetylene to temperatures above 400 °C. A variety of products were produced by this process including benzene, styrene, naphthalene and higher aromatic compounds [12]. In most instances, benzene was the main liquid hydrocarbon produced. Erdmann and Koethner [13] reported that when acetylene is heated with copper metal or copper oxides that cuprene was formed.

The reaction of acetylene with methane to produce propene was investigated by Heinemann [14]. In these reactions, acetylene and methane are heated to 100–200 °C over an alloy catalyst. The alloy consists of one of the metals of iron, nickel, copper, silver or aluminum with one of the metals from the platinum, palladium, iridium group. Winkler and Hauber [15] patented a process where acetylene and olefins are heated in the presence of metallic catalysts to produce dienes and aromatic compounds.

Nieuwland [16] at DuPont discovered one of the earliest commercial uses for acetylene. They found that if monovinylacetylene were treated with hydrogen chloride and the resulting chloroprene polymerized, neoprene would result. DuPont commercialized the process in 1932.

More recent patent literature covers the conversion of acetylene to benzene, styrene, and higher aromatics [17–19]. In the presence of water, a wide range of aliphatics is also formed from the reaction of acetylene. Gasoline may be produced from acetylene by hydroenation to ethylene followed by the Mobil Olefin-to-Gasoline process [20].

2. Experimental

2.1. Acetylene production

2.1.1. Plasma reactor

The configuration of the test apparatus addresses the issues identified as possible causes of measured yields that are smaller than theoretically possible. This configuration includes a four port injector of proven geometry [9], the provision for supersonic expansion through a converging–diverging nozzle to greatly increase quench rates, and a carbon lined reactor which provides residence time for reactions to take place while minimizing radial temperature gradients.

The overall process and instrumentation diagram for the experimental apparatus is shown in Fig. 3. *T* is a temperature, *P* a pressure, FM a flow meter, V a valve, and cw denotes cooling water. A photograph of the test assembly appears in Fig. 4. The detail of the torch, injector, reactor and nozzle assembly appears in Fig. 5, and a photograph of the actual apparatus in Fig. 6. The nozzle assembly could be removed and replaced with a straight copper section of the same inside diameter (i.d.) as the downstream piping to provide baseline data to determine the effectiveness of the aerodynamic quench concept. In addition to the measurements noted on the process and instrumentation diagram, a gas chromatograph is used to analyze the composition of the product stream.

All instrumentation except for the gas chromatograph is directly interfaced to a data acquisition system for continuous recording of system parameters during a test run. Once the specified process power levels, pressures, and gas flow rates are established, the gas stream is continuously sampled by the gas chromatograph for a period of 7 min before the chromatograph gas sample is acquired to ensure that a representative sample is obtained. This sampling period represents approximately three times the time required to completely purge the sample line. The pressure downstream of the quench nozzle is controlled by a mechanical vacuum pump and a flow control valve, V12. Depending on the test conditions, the test pressure can be independently adjusted between atmospheric pressure and approximately 100 Torr. The experiment reaches steady state in a period of 1 min or less. Steady-state operation is verified by a continuously reading residual gas analyzer. All cooling water flow rates and inlet and outlet temperatures are monitored and recorded allowing a complete system energy balance to be calculated. The plasma gases are a mixture of argon and hydrogen; methane or natural gas is injected downstream in a confined channel transverse jet injector. The direct current plasma torch that is currently used will not operate for extended periods of time on pure hydrogen without severe anode erosion, hence all test data is acquired using at least some argon plasma gas. The use of argon, which is inert and does not participate chemically in the process, has the advantage that it provides a built in reference for validating the overall process mass balance. The two most critical aspects of the experiment are the chemical analysis of the product stream and the overall mass balance. These two measurement systems are described separately below.

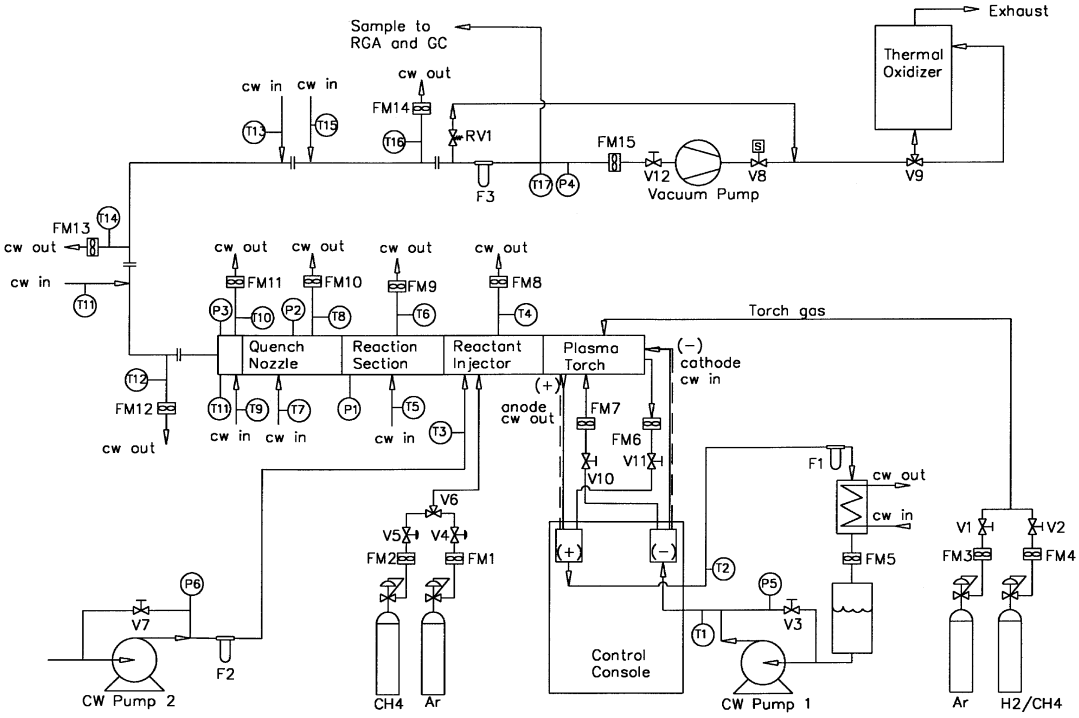

Fig. 3. Process and instrumentation diagram.

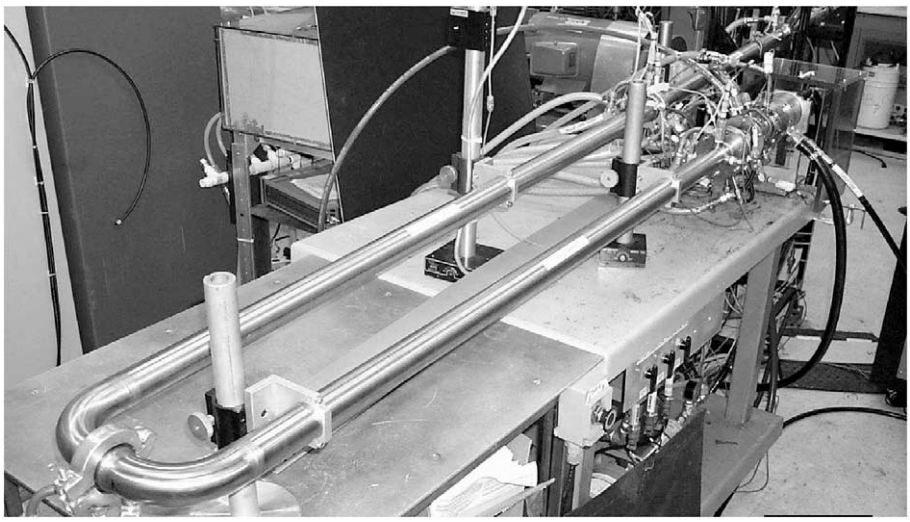

Fig. 4. Photograph of test apparatus.

2.1.2. Mass balance

The flow rates of the feed gases are measured by MKS Model 1559A mass flow controllers. The actual volumetric flow rate of the product gas stream is measured by a Flow Technology Model FT-20AEXA-GEH-1 turbine meter. Because this meter must operate in a reduced pressure environment, a radio frequency pick up is used to avoid the magnetic drag associated with a conventional magnetic pick up. Pressure and temperature were measured just upstream of the turbine meter. In general, the agreement between the MKS mass flow controllers and the downstream turbine meter in cold flow tests with both argon and hydrogen gases was excellent and consistent with the meter specifications. During actual testing, the downstream product volumetric flow rate measurement performed satisfactorily as long as the meter was kept clean. Invariably some ultra fine carbon produced in the experiment would deposit in the meter bearings and cause the meter to under report the actual flow rate; consequently, this data is not always available. The use of argon provided a separate and independent means of estimating product stream volumetric flow rate. Because the argon is inert and does not participate chemically in the overall reaction, the mass flow rate of argon in the produced stream is always the same as the input argon mass flow rate.

2.1.3. Chemical product analysis

The composition of the product stream is analyzed by a Hewlett-Packard Series 6890 Model G1540A gas chromatograph. Because the experiment generally operates at reduced pressure, the sample gas is raised to atmospheric pressure by a stainless steel diaphragm pump. Sample gas continuously flows through the sampling system to the gas chromatograph for a minimum period of 7 min after the experiment has reached steady state. This ensures that a valid and representative sample of the product gas mixture has been obtained. It was found that multi-point non-linear calibrations were required to obtain acceptable measurement performance over the entire range of anticipated tests and associated concentrations. The assigned single sigma measurement uncertainty of $\pm 4\%$ of reading was experimentally determined by repeatedly sampling and analyzing known gas mixtures. Species concentrations measured are shown in Table 2.

2.1.4. Uncertainty estimates

Estimated uncertainties in the primary measurements are summarized in Table 3. From these uncertainty estimates, the system mass balance uncertainties were estimated and are summarized in Table 4.

Independent direct measurement of the amount of solid carbon soot produced is an important component of the validation of the mass balance measurements. It is possible

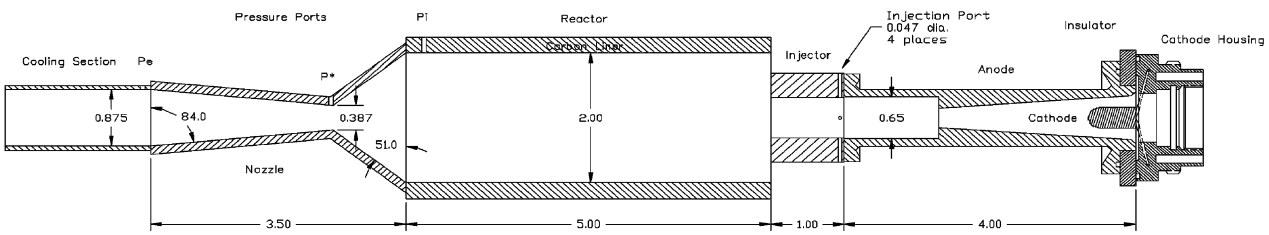

Fig. 5. Schematic of torch, injector, reactor, and nozzle assembly, flow is right to left. All dimensions are in inches.

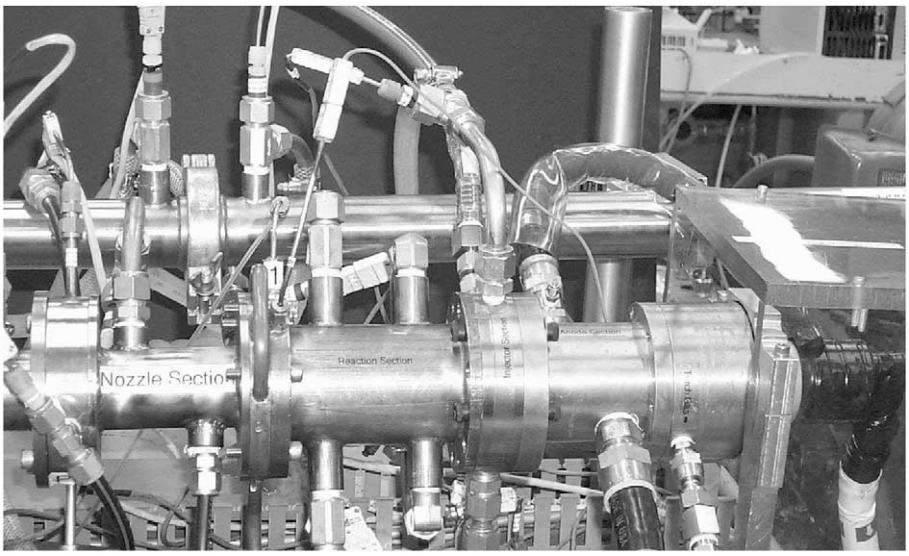

Fig. 6. Photograph of torch, injector, reactor, and nozzle assembly, flow is right to left.

to weigh the downstream filter before and after a run; however, because soot deposits throughout the system, its rate of production is difficult to measure accurately. Two runs were performed to quantify the amount of soot produced. In these runs the entire system was carefully cleaned and the filter and carbon liner in the reactor section weighed. After each nominally 20-min test run, the entire system was again disassembled and the solid carbon removed and weighed, along with the filter and reactor liner. The result of these runs are summarized in Table 5. The yield of solid carbon soot was found to be approximately 4.7% for a methane injection rate of 120.8 standard liters per minute (slm), and 1.9% for a methane injection rate of 98.5 slm. The power level in both runs was 60 kW deposited in the plasma gas.

The overall mass balance measurement performance for an example run is given in Table 6. The largest contributors to the uncertainty in the mass balance measurements are the downstream turbine meter and the gas chromatograph analysis of the product stream. Examination of the table indicates that the measured mass flow rates are within the uncertainty estimates given earlier. This same analysis was applied to each data point acquired. Only those data that demonstrate agreement of the mass balances within the estimated uncertainties were retained.

Table 2
Species concentrations measured

I	Species
1	H_2 (hydrogen)
2	C_6H_6 (benzene)
3	C_3H_8 (propane)
4	C_2H_2 (acetylene)
5	C_3H_6 (propylene)
6	C_4H_{10} (*i*-butane)
7	C_3H_4 (propadiene)
8	C_4H_{10} (*n*-butane)
9	C_4H_8 (1-butene)
10	C_4H_8/C_4H_{10} (*i*-butylene/*i*-butane)
11	C_4H_8 (*t*-2-butene)
12	C_4H_8 (*c*-2-butene)
13	C_4H_6 (1,3-butadiene)
14	C_5H_{12} (*i*-pentane)
15	C_5H_{12} (*n*-pentane)
16	CO_2 (carbon dioxide)
17	C_2H_4 (ethylene)
18	C_2H_6 (ethane)
19	Ar (argon)
20	N_2 (nitrogen)
21	CH_4 (methane)
22	CO (carbon monoxide)

2.2. Conversion of acetylene

The single-component catalysts were used as received without any further purification. The supported metal catalysts were prepared by dissolving the metal salt in water and mixing the resulting solution with the support. After several hours of mixing, the water was removed under reduced pressure. The resulting solid was dried in a vacuum oven at 95–110 °C overnight.

Table 3
Summary of estimated uncertainties in primary measurements

Quantity	Uncertainty type, range or reading (%)	Assigned 1σ uncertainty
Temperature	–	±1 °C
Pressure	Range	±0.5%
Product volumetric flow rate	Range	±5%
Plasma gas volumetric flow rate	Range	±1%
Reactant gas volumetric flow rate	Range	±1%
GC molar concentration	Reading	±4%

Table 4
Estimated uncertainties in derived quantities

Derived quantity	2σ Uncertainty estimate using turbine meter to measure product volumetric flow rate (%)	2σ Uncertainty estimate using argon concentration to estimate product volumetric flow rate (%)
Product volumetric flow rate, $\dot{Q}_{STP}$ or $\dot{Q}_{STP(Ar)}$	6.1	4.1
Methane yield, y_{CH_4}	7.4	5.8
Conversion efficiency, CE	3.1 (maximum)	2.5 (maximum)
Acetylene yield, $y_{C_2H_2}$	7.4	5.8
Product stream total mass flow rate, $\dot{m}_t$	7.3	5.7
Product stream carbon mass flow rate, $\dot{m}_C$	7.3	5.7
Product stream hydrogen mass flow rate, $\dot{m}_H$	7.3	5.7

Table 5
Rate of production and yield of solid carbon soot

Argon (slm)	Hydrogen (slm)	Methane (slm)	Solid carbon produced (g/min)	Solid carbon yield (%)
140	100	98.5	1.03	1.9
140	100	120.8	3.02	4.7

Heating the supported metal salt in a stream of hydrogen at 500 °C for 8 h reduced the metal salt to the supported metal.

All experiments were conducted in a 0.5 in. outside diameter (o.d.) × 0.375 in. i.d. [1.27 cm o.d. × 0.95 cm i.d.] × 10 in. (25.4 cm) 304 stainless steel reactor. The inside wall of the reactor was coated with Restek Corporation's Sikasteel® coating. The catalyst (1 g) was supported in the reactor on a deactivated quartz-wool plug. The reactor was operated in an up-flow configuration. A gold-plated thermocouple in the center of the catalyst bed was used to control the temperature of reaction to ±0.5 °C. Brooks proportional ratio mass-flow controllers were used to control the feed of gases to the reactor. An Isco high-pressure syringe pump was used to control the feed of liquids to the reactor. The reactants were preheated to approximately 130 °C prior to entering the reactor and the products of reaction were heated to approximately 175 °C between the exit of the reactor and the cold trap, which was maintained at −4 °C.

Products of reaction were directly sampled and analyzed after 1 h of reaction by an online dual-column gas chromatograph. The gas chromatograph, a Hewlett-Packard™ 5890 Series II, was equipped with a 100 m × 0.25 mm i.d. fused silica column coated with 0.5 μm film of 100% dimethylpolysiloxane (Petrocol DH obtained from Supelco) and a 50 m × 0.32 mm porous layer open tubular (PLOT) column containing Al_2O_3/KCl (obtained from Chrompack). The gas chromatograph was temperature programmed at 1 °C min^{-1} from 30 to 200 °C. Helium was used as the carrier gas having an average linear velocity, at 30 °C, of 41 ml min^{-1} for the Petrocol column and 32 ml min^{-1} for the PLOT column. The Petrocol column was used to separate the liquid components of reaction while the PLOT column was used to separate the gaseous components. Dual flame ionization detectors were employed to detect the separated components. When possible, the products were also analyzed by an online quadrupole mass spectrometer connected to the exhaust line upstream of the gas chromatograph.

3. Results and discussion

3.1. Acetylene production

Two primary test series were conducted with the major difference between the two being the presence or absence of the converging–diverging quench nozzle. When the quench nozzle is installed, the downstream valve, V12, is wide open and the downstream pressure is determined by the capacity of the vacuum pump. The downstream pressure in this mode generally runs between 100 and 200 Torr. In this configuration, the flow is choked in the converging–diverging nozzle throat and the reactor pressure is determined by the nozzle throat diameter, the reactor temperature, and the mass flow rate of the plasma and reactant gases. Under these conditions, the reactor pressure generally ran between 600 and 800 Torr for an upstream to downstream pressure ratio between 4 and 6. The corresponding Mach number range is 1.6–1.8. Assuming a reactor temperature of 2000 °C, the aerodynamic quench rapidly lowers the temperature to 1100–1300 °C. The measured thermal efficiency of the plasma torch was between 80 and 90% depending on the gas mixture and flow rates. The power

Table 6
Example of mass balance performance, 140 slm Ar, 100 slm H_2, 120.8 slm CH_4

Mass component	Input (g/min)	Product stream			
		Turbine meter		Argon flow rate	
		Measured (g/min)	Error (%)	Measured (g/min)	Error (%)
Total, $\dot{m}_t$	345.21	343.2	0.58	352.47	−2.10
Carbon, $\dot{m}_C$	64.71	68.94	−6.54	70.81	−9.42
Hydrogen, $\dot{m}_H$	30.5	30.73	−0.75	31.56	−3.47
Argon, $\dot{m}_{Ar}$	250.0	243.42	2.63	250	0
Carbon soot, $\dot{m}_{C(S)}$	3.02 (measured)	−4.23[a]	–	−6.1[a]	–

[a] Estimated from the difference of the carbon in the product stream and the input value. Since the uncertainty in the measured value is of the same order of magnitude as the difference, the uncertainty in the result is necessarily large.

to the plasma torch was adjusted to give a constant 60 kW deposited in the plasma gas. Since the torch voltage is essentially determined by the argon to hydrogen ratio, the power was adjusted by adjusting the current to obtain the desired 60 kW into the plasma. The injector ring, reactor section, and nozzle assembly, Fig. 5, energy balances indicated that approximately 14.6 kW were lost in these components to the cooling water. The partitioning of this energy loss is illustrated in Fig. 7.

Fig. 7 shows that approximately 45 kW is available for conversion of natural gas to acetylene. By careful system redesign, which includes placement of the injector function inside the torch body and optimization (shortening) of reactor length, these losses can probably be reduced by 70% or more. The target reactor temperature is 2000 °C. Under the nominal operating conditions (target reactor temperature of 2000 °C, 160 slm argon, 100 slm hydrogen for the plasma torch gas and 60 kW deposited in the plasma), the maximum theoretical amount of methane that can be converted to acetylene is approximately 145 slm.

3.1.1. Results with converging–diverging nozzle

CE as a function of the rate of methane injection is plotted in Fig. 8. CE is simply the percentage of methane in the fed stream converted to another product. In developing this data set the power deposited in the plasma was maintained constant at 60 kW and the plasma gas flow rates were constant at 160 slm argon and 100 slm hydrogen. The measured reactor pressure was relatively constant, varying between approximately 670 and 730 Torr, depending on the rate of methane injection. Methane conversion is essentially complete, that is a CE of 100%, at methane feed rates up to about 100 slm. At feed rates above 100 slm, the CE starts to decline. The estimated bulk gas temperature in the reactor and corresponding residence time in the reactor is plotted in Fig. 9. This estimate is obtained from the measured system energy balance, the plasma gas and methane flow rates, and the assumption of 100% acetylene yield. The target temperature of approximately 2000 °C is reached at a methane flow rate of approximately 145 slm. For methane injection rates less than 145 slm, the estimated reactor temperature is greater than 2000 °C. For injection rates in excess of 145 slm, there is not enough energy available to dissociate and convert the injected methane to acetylene with 100% efficiency and result in a product stream temperature of 2000 °C. The presence of the inevitable cold boundary layers in the injection ring and reactor also result in some gas that can pass through the reactor without being dissociated. At the lower flow rates and corresponding higher temperatures, the methane is almost completely converted and the CE approaches 100%. The CE is observed to decline at 120 slm, somewhat below the anticipated value of 145 slm. This may be due to the presence of cold boundary layer flow, or due to inadequate residence time for dissociation. Inspection of the residence time plot in Fig. 9 shows that the residence time in the reactor is relatively constant and independent of methane injection rate. The increase in mass flow rate and anticipated velocity increase with increased methane injection is offset by the cooling of the gas mixture that also occurs with increased methane injection rate.

The possible influence of residence time on CE was evaluated by replacing the converging–diverging nozzle with a straight, constant diameter section that matched the inside diameter of the downstream piping. By removing the converging–diverging nozzle, the reactor pressure could be controlled independently of the flow rates. When the converging–diverging nozzle is installed, the flow is choked

Torch	Injector	Reactor	Nozzle
+60 kW into plasma	-7.3 kW to cooling water	-3.9 kW to cooling water	-3.4 kW to cooling water

Fig. 7. Partitioning of energy loss to cooling water.

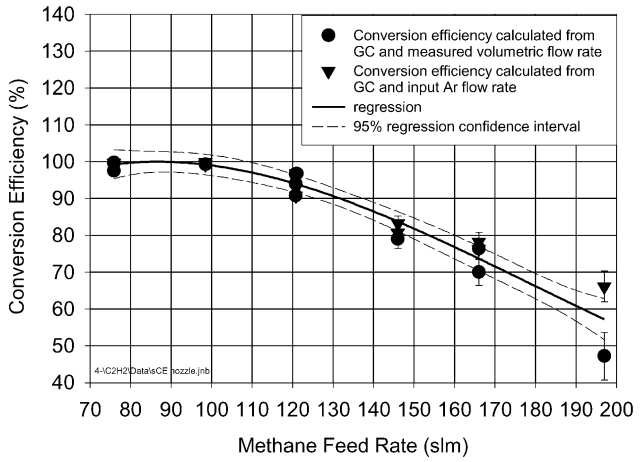

Fig. 8. CE as a function of methane feed rate, plasma power is constant at 60 kW, and plasma gas flow rates are constant at 160 slm argon and 100 slm hydrogen.

(reaches sonic velocity) in the nozzle throat. Under this condition the reactor pressure is independent of the downstream pressure and is determined solely by the mass flow rate and temperature. With the converging–diverging nozzle removed, the reactor pressure is controlled by the position of a downstream valve. Decreasing the reactor pressure increases the velocity in the reactor and decreases residence time. For this series of tests the pressure was varied from 300 to 700 Torr, decreasing the residence time in the reactor by a factor of 2.3, or from about 3.25–1.4 ms. A slight decrease in CE of about 2% points, is observed at the lower pressures, Fig. 10. While this suggests a slight dependence on residence time, it is not enough to account for the decrease in CE observed in Fig. 8. This suggests that the presence of cold boundary layers is in fact mostly responsible for the observed decrease. The residence time in the reactor is sufficient for dissociation of the methane, and as we will show next, also sufficient for the formation of acetylene.

Acetylene yield as a function of methane injection rate

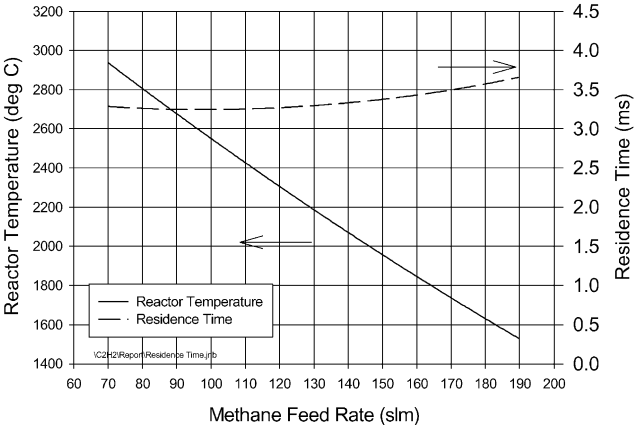

Fig. 9. Estimated reactor temperature and reactor residence time as a function of methane injection rate.

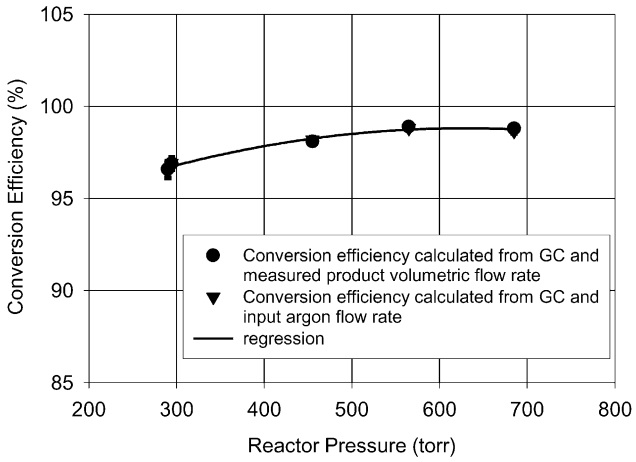

Fig. 10. Methane CE as a function of reactor pressure.

appears in Fig. 11. The trends observed in the yield data are similar to those observed in the plot of CE, Fig. 8. The acetylene yield is approximately 95% for methane injection rates less than about 100 slm. Further increases in methane injection rate result in a decrease of yield. At an injection rate of 145 slm, the theoretical maximum feed rate that can be processed with CE and yield approaching 100%, the measured yield has dropped to 75%. In Fig. 12, the measured yield has been normalized to account for the measured decrease in CE. This normalization is simply $\text{yield}_{\text{normalized}} = \text{yield/CE}$.

The normalized yield is a measure of selectivity for conversion to acetylene. As shown in Fig. 12, this normalization accounts for a significant portion of the observed decrease in acetylene yield. Improving the CE will flatten the yield curve significantly. This suggests that minimization of the cold boundary layers through improved thermal design can result in an improvement in overall system performance and that the intrinsic acetylene yield is high over a wide range of reactant flow rates (reactor temperature).

The decrease in the measured yield that is not accounted

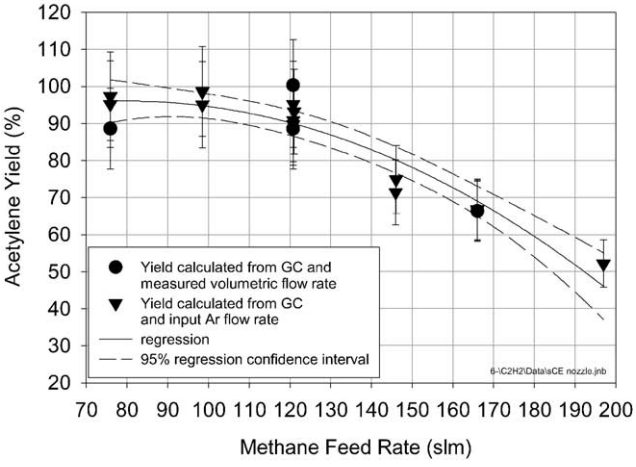

Fig. 11. Acetylene yield as a function of methane injection rate.

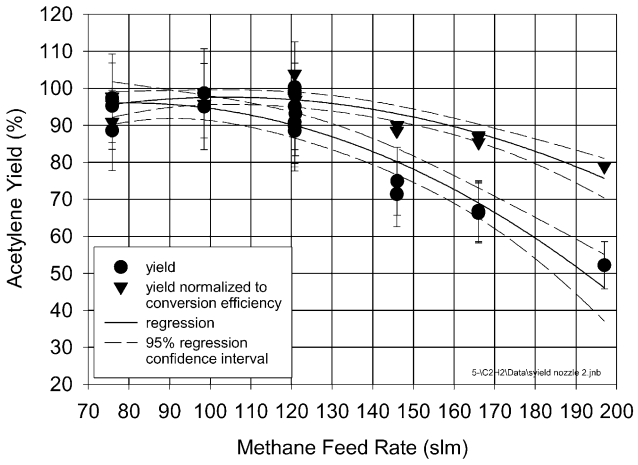

Fig. 12. Normalized acetylene yield.

for by the decrease in CE is due to the formation of other carbon containing species. These include other hydrocarbons and soot. Fig. 13 contains plots of the carbon basis yield of the other hydrocarbon species observed as a function of methane injection rate. Yield is given as a percentage of carbon introduced into the system as methane. The observed decrease in the normalized acetylene yield is due to an increase in the yield of other carbon containing species. The species represented on the plot are the only ones observed by the gas chromatograph. Interestingly enough, after an initial increase in the yield of olefins plus the C_6 and heavier ($C_5 = /C^6+$) hydrocarbons the relative amount decreases slightly at higher methane injection rates. The $C_5 = /C^6+$ gas chromatograph peak was subsequently identified as almost entirely benzene by gas chromatography–mass spectrometry analysis.

In addition to the tests utilizing methane as the reactant gas, a limited number of runs were performed using pipeline natural gas. The observed conversion efficiencies, acetylene yields and the yields of other hydrocarbons were identical to the prior results using pure methane as the feedstock. The results were virtually identical to the pure methane runs with the exception of N_2, which is essentially inert, and the

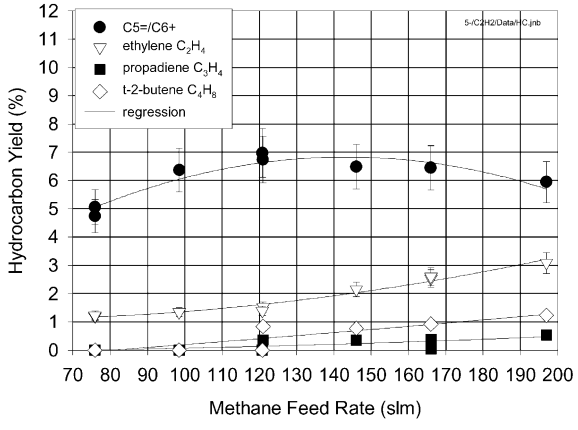

Fig. 13. Yield of all other observed hydrocarbons less methane.

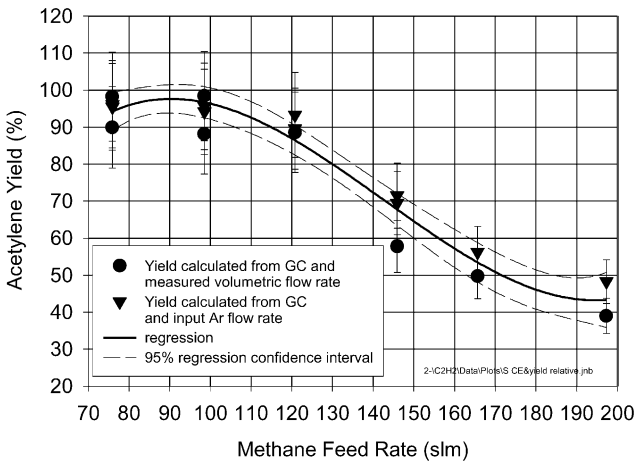

Fig. 14. Acetylene yield as a function of methane injection rate. The converging–diverging nozzle has been removed.

conversion of the carbon dioxide (CO_2) to carbon monoxide (CO).

3.1.2. Results without converging–diverging nozzle

The CE (~100 vs. 70%), yield, and selectivity (95 vs. 51%) of the process demonstrated appear to be superior to the original Hüels process. The Hüels feed and product stream analyses as well as the INEEL results are summarized in Table 7. This may be due to better mixing, temperature uniformity, or more rapid quenching. To assess the effect of rapid aerodynamic quenching a series of tests, identical to those reported earlier, were conducted but without the converging–diverging nozzle. In these tests, the system pressure was maintained at between 700 and 900 Torr, approximately the same as the reactor pressure in the first test series.

The yield (Fig. 14) and CE results without the converging–diverging nozzle and supersonic aerodynamic quench are virtually identical to the earlier results developed with the nozzle present. There appears to be some minor improvement in yield at the higher methane injection rates when the nozzle is present (Fig. 14 vs. Fig. 11), but the deviations are within the uncertainty estimate and the error bars significantly overlap. Examination of yields of other hydrocarbons, Fig. 15, indicate a statistically significant difference in the yield of ethylene between the results with the nozzle removed and with the nozzle in place, Fig. 13. Apparently the high quench rates afforded by the nozzle have the effect of suppressing the formation of ethylene, cutting the yield of ethylene by approximately one-third. The exact mechanism of ethylene formation is as yet undefined; however, it is likely that the kinetics and population of the CH_2 radical play an important role.

With the converging–diverging nozzle removed, the reactor pressure can be independently controlled with valve V12. This configuration allows investigation of the effect of pressure on yield. It was demonstrated earlier, Fig. 10, that pressure and residence time have only a

Table 7
Product stream analysis in mole percent

		Acetylene, C_2H_2	Allene, C_3H_4	Diacetylene, C_4H_2	C_4H_4	Ethylene, C_2H_4	Methane, CH_4	Ethane, C_2H_6	Propane, C_3H_8	*i*-Butane, C_4H_{10}	*n*-Butane, C_4H_{10}	Benzene, C_6H_6	H_2	CO	N_2	Carbon yield (%)
Hüels process	Feedstock	–	–	–	–	–	92.3	1.4	0.5	–	0.4	–	–	–	5.4	–
	Product	14.5	0.4	0.6	0.1	0.9	16.3	0.04	0.03	0.01	–	0.3	63.4	0.6	2.7	2.7
Current process *w*/quench	Feedstock	–	–	–	–	–	93.47	3.79	0.74	0.10	0.11	0.04	–	–	1.18	–
	Product[a]	11.8	–	–	–	–	0.21	–	–	–	–	0.34	53.47	0.25	0.44	3.2

[a] Also includes 33.3 mol% Ar.

small effect on CE. Measured acetylene yield is plotted as a function of reactor pressure in Fig. 16. The power is constant at 60 kW into the gas and the flow rates are maintained at 160 slm argon, 100 slm hydrogen, and 98.5 slm CH_4. There appears to be a slight decrease in acetylene yield with increasing pressure although the effect is not large. The decrease in yield is accompanied by a slight decrease in benzene yield and an increase in ethylene yield, Fig. 17. In general, pressure changes in the range of 300–700 Torr do not have a large effect.

The measured CE and acetylene yield in the laboratory reactor system described here are in general somewhat better than reported in the literature; conversion efficiencies approach 100% and yields in the 90–95% range with 2–4% soot produced have been demonstrated. This appears to be somewhat of an improvement over the Hüels process (CE = 70.5% and $YC_2H_2 = 51.4$, 2.7% carbon soot) and the DuPont process (CE, not reported; $YC_2H_2 = 70\%$). The process reported here also appears to have somewhat better specificity for acetylene. The improvement in CE, yield and specificity are due primarily to improved injector design and mixing (a better 'stirred' reactor) and minimization of temperature gradients and cold boundary layers. The rate of cooling by wall heat transfer appears to be sufficient to quench the product stream and prevent further decomposition of acetylene into soot or further reaction leading to heavier hydrocarbon products. Significantly increasing the quench rate by rapidly expanding the product stream through a converging–diverging nozzle leads to only marginal improvement in the composition of the product stream, primarily the reduction of the yield of ethylene.

The specific amount of energy consumed (kW h) per amount (kg) of acetylene produced ultimately determines the economics of the process. The Hüels process reportedly consumed 12.1 kW h kg^{-1} C_2H_2 produced. The DuPont process specific energy consumption was estimated, though not measured, to be 8.8 kW h kg^{-1} C_2H_2 produced. This later value compares favorably with the theoretical minimum value of approximately 7.9 kW h kg^{-1} C_2H_2 for a product stream at 2000 °C, 100% CE and yield and no electrical or thermal losses. The measured specific energy consumption for the laboratory scale process examined in this study is plotted in Fig. 18. The minimum measured specific energy consumption is approximately 16 kW h kg^{-1} C_2H_2 produced. It is estimated that this could be improved to a value of around 13 kW h kg^{-1} C_2H_2 by improved thermal design. This includes moving the injection into the torch body thus avoiding the thermal losses in the injector ring and reducing the thermal losses in the reactor section. Process heat recovery might further reduce the specific energy consumption by another 20% or so to around the 10 kW h kg^{-1} C_2H_2 range. These numbers compare favorably with the specific energy consumption reported for the Hüels and DuPont processes while demonstrating improved CE and yield.

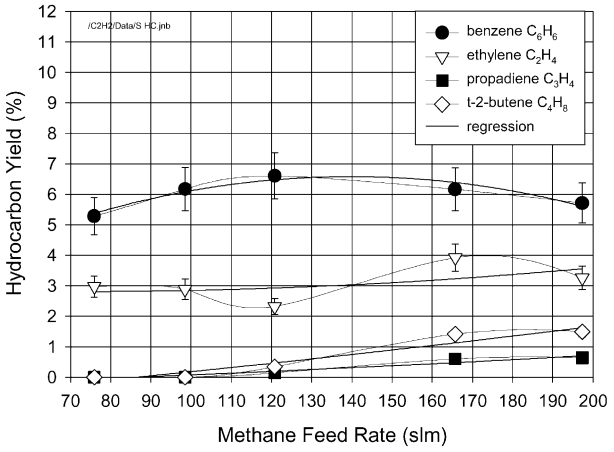

Fig. 15. Yield of all other observed hydrocarbons, less methane. The converging–diverging nozzle has been removed.

3.2. Conversion of acetylene

Reactions of acetylene were conducted neat and mixed with methanol, methane, hydrogen, carbon monoxide, and carbon dioxide with limited success. In all instances, total conversion of acetylene could be achieved by elevating the reaction temperature. In these instances, the major product was coke. In some instances, the quantity of coke produced was so large that the reactor became plugged. By proper selection of catalyst and reaction condition, conversions of acetylene could be conducted with an acceptable level of conversion and limited benzene and coke production.

3.2.1. Conversion of acetylene alone

The reaction of acetylene over a shape-selective aluminosilicate zeolite resulted in the low conversion of acetylene. Reactions were conducted at temperatures between 200 and 350 °C. Conversions of acetylene were 6% at 200 °C increasing to 15% at 350 °C. The main products of reaction were methane and coke. Table 8 lists the non-coke products as a function of temperature.

This reaction results in the stoichiometric dissociation of acetylene. Methane comprised the largest amount (>88 wt%)

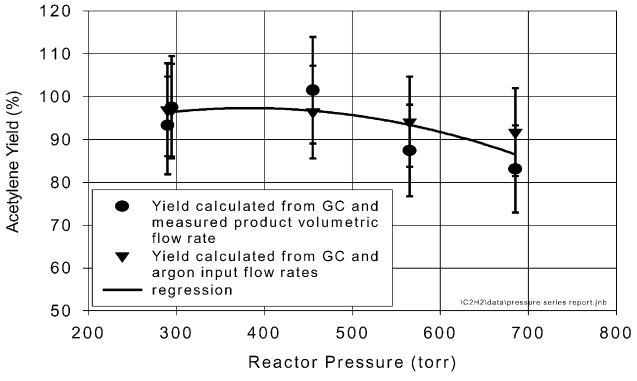

Fig. 16. Acetylene yield as a function of pressure, converging–diverging nozzle removed, 160 slm argon, 100 slm hydrogen, 98.5 slm CH_4.

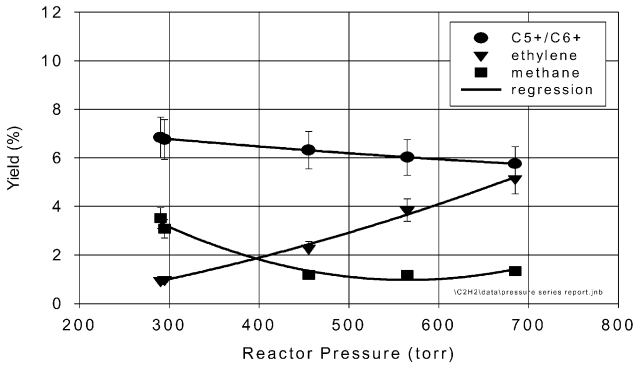

Fig. 17. Hydrocarbon yield as a function of reactor pressure.

of the non-coke product. At all temperatures (except 200 °C), the main product other than methane or coke was propane (between 0.78 and 1.60 wt%). The drop in conversion at 250 and 300 °C is most likely due to rapid plugging of the zeolite's pores by coke. At 350 °C, we observed an increase in acetylene conversion. At 200 °C, benzene was the main product after coke and methane. As the temperature of reaction increased, the production of aromatics also increased. As is shown in Table 8, aromatic compounds containing up to 10 carbon atoms were observed.

3.2.2. Conversion of acetylene with methane

A US Patent by Heinemann [14] reported that the reaction of acetylene and methane over supported metal catalysts produced propylene in 70% yield. While propylene is not a liquid at room temperature, it can be converted by contact with a shape-selective zeolite to produce gasoline-range hydrocarbons. We investigated the reaction of acetylene and methane using a variety of catalysts. These included tungsten oxide, titanium dioxide, silicon dioxide, alumina, copper on silica, copper on titania, and nickel on silica. All of these catalysts exhibited similar results, acetylene conversion is relatively high (with the exception of silicon dioxide) and the reaction produces more methane than is consumed. The results are listed in Table 9. The main products of reaction in all cases were methane and coke.

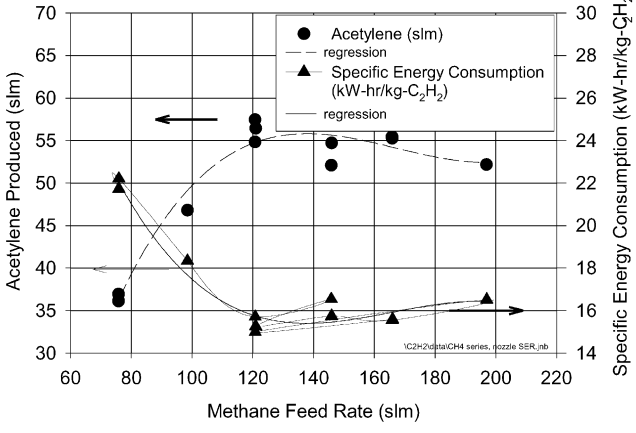

Fig. 18. Specific energy consumption.

Table 8
Conversion and normalized weight percent of products from the reaction of acetylene over a zeolite

Compound (wt%)	Temperature (°C)			
	200	250	300	350
Acetylene conversion (%)	5.96	3.28	3.90	15.28
C1	98.87	97.59	96.74	87.98
C2	0.00	0.00	0.00	0.00
C2 =	0.00	0.00	0.00	0.00
C3	0.21	0.78	1.20	1.60
C3 =	0.00	0.00	0.00	0.00
C4	0.05	0.08	0.14	0.16
C4 =	0.02	0.21	0.42	0.75
C5 + aliphatic	0.01	0.45	0.69	3.87
A6	0.40	0.17	0.14	0.74
A7	0.15	0.18	0.19	0.85
A8	0.17	0.23	0.27	0.89
A9	0.09	0.18	0.20	1.14
A10	0.04	0.14	0.01	1.21
A11 +	0.00	0.00	0.00	0.83

The amount of coke produced when acetylene and methane were reacted over the supported copper catalysts was so great that the reactor could not be removed from the outlet transfer line.

3.2.3. Conversion of acetylene with oxygen-containing compounds

Reppe and Wolfe [21] reported that acetylene and methanol could be reacted at relatively low (<150 °C) temperatures to produce 1,1-dimethoxyethane. A liquid at room temperature, 1,1-dimethoxyethane can be used as a cetane enhancer in diesel fuel. In our experiments, acetylene and methanol at $1\ h^{-1}$ weight hourly space velocity (WHSV) each were passed over soda lime at 100 and 150 °C for extended periods of time. The results of these experiments are listed in Table 10.

Acetylene conversion was low at 100 °C, 7.18% while methanol conversion was high, 78.34%. At 150 °C, conversion of acetylene increased to 29.2% while methanol conversion dropped to 48.89%. The major products of reaction were 1,1-dimethoxyethane and methane. Of note is the lack of aromatics in the product stream.

The reaction of acetylene and oxides of carbon (carbon monoxide and carbon dioxide) was conducted over the zeolite catalysts. Reactions were conducted at temperatures between 200 and 350 °C. Conversions and product selectivities are listed in Table 11.

As is shown in Table 11, at low temperatures the main product of reaction is methane. As the temperature of reaction increases, the production of methane decreases as other products are produced. When acetylene is reacted with carbon monoxide at 300 °C, the main product of reaction is toluene, followed by propane, benzene, and butane. The results of the reaction of acetylene and carbon dioxide are different than those observed for the reaction of acetylene and carbon monoxide. At higher temperatures, the main products of reaction are ethylene, butane, and butene. Only small quantities of aromatics were detected in the reaction of acetylene and carbon dioxide.

3.2.4. Conversion of acetylene with hydrogen

The plasma reactor produces hydrogen along with acetylene. The hydrogen can be used to hydrogenate the acetylene to produce ethylene, a valuable industrial starting material. However, ethylene does not meet the criteria of being a liquid at room temperature and therefore, cannot be transported utilizing existing infrastructures. The reaction of acetylene and hydrogen over the shape-selective zeolite exhibited the most promising of all reactions that we

Table 9
Conversion and normalized weight percent of products from the reaction of acetylene and methane at 300 °C over various catalysts

Compound (wt%)	WO_3	TiO_2	SiO_2	Al_2O_3	Cu/TiO_2	Cu/SiO_2	Ni/SiO_2
Acetylene conversion (%)	15.28	16.19	6.30	11.05	87.29	100	25.10
Methane conversion (%)	−1.90	−62.45	−4.38	−6.41	−30.29	−39.97	−14.98
C1[a]	97.40	91.68	99.03	99.19	88.75	94.10	98.13
C2	0.00	0.00	0.00	0.00	0.00	0.91	0.00
C2 =	0.00	0.00	0.00	0.00	0.00	0.00	0.00
C3	0.00	0.70	0.00	0.00	0.01	0.79	0.00
C3 =	0.00	0.00	0.00	0.00	0.00	0.00	0.00
C4	0.42	0.47	0.01	0.00	0.33	0.19	0.03
C4 =	0.17	1.16	0.06	0.00	5.24	0.57	0.13
C5 + aliphatic	1.80	3.55	0.88	0.80	4.13	1.75	1.45
A6	0.19	1.07	0.01	0.00	1.31	0.14	0.25
A7	0.00	0.01	0.00	0.00	0.00	0.43	0.00
A8	0.01	0.44	0.00	0.00	0.22	0.56	0.00
A9	0.00	0.23	0.00	0.00	0.01	0.41	0.00
A10	0.01	0.39	0.00	0.00	0.00	0.15	0.00
A11 +	0.00	0.30	0.00	0.00	0.00	0.00	0.00

[a] Does not include unreacted methane.

Table 10
Conversion and normalized weight percent of products from the reaction of acetylene and methanol over soda lime

Compound (wt%)	Temperature (°C)	
	100	150
Acetylene conversion (%)	7.18	29.2
Methanol conversion (%)	78.34	48.89
C1	15.24	36.37
C2	0.00	0.16
C2 =	0.00	0.00
C3	0.00	0.00
C3 =	0.00	0.00
C4	0.19	0.15
C4 =	0.00	0.00
C5 + aliphatic	6.39	1.85
A6	0.00	0.01
A7	0.00	0.00
A8	0.00	0.00
A9	0.00	0.00
A10	0.00	0.00
A11 +	0.00	0.00
1,1-Dimethoxy-ethane	78.18	61.47

investigated. Acetylene and hydrogen, at 1 h^{-1} WHSV each and 1 and 2 h^{-1} WHSV, respectively, were reacted over the zeolite at various temperatures. The results of the reactions are listed in Tables 12 and 13.

With the equal molar quantities of acetylene and hydrogen as reactants, the main products of reaction at low temperature are methane and benzene. Conversion of acetylene increases with increasing temperature, from an almost undetectable value at 200 °C to ~58% at 350 °C. As the temperature increases, the production of methane passes through a minimum around 300 °C. The production of benzene decreases as the temperature increases. At higher temperatures the production of higher aromatic compounds increases, however, they are not the main products of reaction. The main products are methane, propane, butane, butene, and C_5+ aliphatics. As the temperature of reaction increased, the production of coke also increased.

The reaction of acetylene with excess hydrogen produced similar results as those observed for the equimolar reactions (Table 13). A notable exception is that the reaction of acetylene with excess hydrogen was observed to occur at temperatures as low as 50 °C. As the temperature of reaction increased the conversion of acetylene increases reaching a plateau between 200 and 300 °C. Increasing the reaction temperature from 300 to 350 °C resulted in the conversion of acetylene increasing threefold. Methane production passes through a minimum around 150 °C. With the excess hydrogen present, the production of aromatics is lower than that observed in the equimolar reactions.

4. Conclusions

4.1. Acetylene production

1. Improvements in process CE and acetylene yield over prior art are possible. The improvements are primarily accomplished by more efficient injection and mixing of reactants with plasma gases and minimization of temperature gradients and cold boundary layers in the reactor.
2. Improved mixing and thermal control also leads to increased specificity reducing the yield of hydrocarbons other than acetylene.

Table 11
Conversion and normalized weight percent of products from the reaction of acetylene with carbon oxides

Compound (wt%)	*w*/CO			*w*/CO_2			
	Temperature (°C)						
	200	250	300	200	250	300	350
Acetylene conversion (%)	0.01	60.00	100	10.50	10.80	4.60	16.80
C1	92.31	69.84	4.76	93.71	21.03	19.95	26.14
C2	0.00	0.00	0.00	0.00	0.00	0.00	0.00
C2 =	0.00	0.00	0.00	5.38	6.78	20.20	36.85
C3	1.94	5.40	17.72	0.00	0.00	0.00	4.21
C3 =	0.00	0.00	0.00	0.00	0.00	0.00	0.00
C4	0.00	4.14	11.55	0.23	34.98	11.16	15.37
C4 =	0.07	0.42	3.96	0.68	0.00	6.69	11.26
C5 + aliphatic	0.54	5.79	6.66	0.00	36.53	41.11	3.08
A6	5.15	8.91	11.57	0.00	0.66	0.89	2.40
A7	0.00	0.00	43.78	0.00	0.00	0.00	0.00
A8	0.00	5.51	0.00	0.00	0.00	0.00	0.34
A9	0.00	0.00	0.00	0.00	0.00	0.00	0.10
A10	0.00	0.00	0.00	0.00	0.00	0.00	0.24
A11 +	0.00	0.00	0.00	0.00	0.00	0.00	0.00

Table 12
Conversion and normalized weight percent of products from the reaction of acetylene with hydrogen

Compound	Temperature (°C)			
	200	250	300	350
Acetylene conversion (%)	0.02	8.51	15.57	57.93
C_2H_2:H_2	1:1			
wt%				
C1	64.23	26.91	18.82	44.60
C2	0.00	0.00	0.00	0.00
C2 =	0.00	0.00	0.00	0.00
C3	0.00	4.75	10.48	5.72
C3 =	0.00	0.00	0.00	0.00
C4	8.46	20.00	32.37	10.98
C4 =	1.15	23.88	17.13	8.74
C5 + aliphatic	2.69	12.23	11.93	17.73
A6	23.46	9.64	5.40	3.73
A7	0.00	2.59	3.79	2.12
A8	0.00	0.00	0.08	1.79
A9	0.00	0.00	0.00	1.48
A10	0.00	0.00	0.00	1.27
A11 +	0.00	0.00	0.00	1.85

3. The quench rate achieved by wall heat transfer in small reactors is adequate to arrest acetylene decomposition and soot formation. Quench rates by wall heat transfer are estimated to be on the order of 0.1×10^6 °C s^{-1}.
4. Formation of other hydrocarbon species, except for ethylene, is unaffected by significantly increasing the quench rate.
5. The yield of ethylene can be minimized through the addition of the aerodynamic quench process, although the effect on acetylene yield is small.
6. While performance enhancements by greater quench rates are marginal in small reactors, larger scale devices may benefit from quench rate enhancements.
7. While greater product selectivity for acetylene has been demonstrated, the specific energy consumption has not been improved upon. Greater specificity may reduce costs by simplifying separation product separation requirements; however, the fundamental specific energy consumption for conversion of natural gas to acetylene is on the order of 10 kW h kg^{-1} C_2H_2.

The next steps towards commercialization of the improved plasma process for the conversion of methane to acetylene are as follows:

- Demonstrate operation with methane torch gas using advanced torch technology to allow extended electrode lifetimes and elimination of argon torch gas.
- Establish and correct the major sources of energy inefficiencies.
- Engineer and build an integrated reactor system to benchmark energy efficiency and electrode lifetime expectations.
- Characterize the carbon produced and determine its economic value (which will have a minor effect on the economics of the process).

4.2. Conversion of acetylene

While methane can be efficiently converted to acetylene, the further conversion to liquid fuels must be further developed for the methane to acetylene process to play an important role in dealing with remote natural gas.

We investigated several different conversion technologies for acetylene. Acetylene was reacted by itself or with methanol, methane, carbon monoxide, carbon dioxide, or hydrogen over a variety of catalysts. In most instances, the main products of reaction were to benzene, methane, or coke. The production of 1,1-dimethoxyethane from acetylene and methanol occurred with acceptable conversions and

Table 13
Conversion and normalized weight percent of products from the reaction of acetylene with hydrogen

Compound (wt%)	Temperature (°C)							
	50	75	100	150	200	250	300	350
Acetylene conversion (%)	2.08	2.89	5.83	10.87	18.31	13.77	14.00	40.39
C_2H_2:H_2	1:2							
C1	16.39	13.95	8.15	3.53	23.61	6.84	18.09	57.71
C2	0.00	0.00	0.00	0.00	0.00	0.00	0.00	0.00
C2 =	0.00	0.00	0.00	0.00	0.00	0.00	0.00	0.00
C3	5.79	5.87	4.67	3.81	4.86	9.84	9.87	8.47
C3 =	0.00	0.00	0.00	0.00	0.00	0.00	0.00	0.00
C4	2.07	3.18	4.36	2.86	2.42	33.90	23.25	3.82
C4 =	43.46	43.23	45.77	49.71	35.96	8.85	7.17	11.31
C5 + aliphatic	30.22	31.28	32.72	33.50	29.86	36.25	33.13	11.67
A6	2.07	2.07	2.83	5.09	1.95	2.40	2.53	2.97
A7	0.00	0.41	0.46	0.39	0.42	0.78	1.18	2.03
A8	0.00	0.00	1.03	1.12	0.92	1.15	1.90	0.91
A9	0.00	0.00	0.00	0.00	0.00	0.00	1.74	0.66
A10	0.00	0.00	0.00	0.00	0.00	0.00	1.15	0.45
A11 +	0.00	0.00	0.00	0.00	0.00	0.00	0.00	0.00

yields. Conversions of acetylene and methanol at 150 °C were 29.20 and 48.89%, respectively. The main products of reaction were 1,1-dimethoxyethane and methane. The problem with this technology at a remote location is the need for methanol as a reactant. If methanol is produced from methane at the location, the methanol (a liquid at room temperature) can be transported to market directly. This eliminates the need for acetylene production and conversion. The reaction of acetylene with a twofold excess of hydrogen over a shape-selective zeolite proved the most promising technology. Conversions of acetylene, at relatively low temperatures, of ~20% were observed. The product slate consisted of C_3–C_5 + aliphatics with less than 4% aromatic content.

5. Disclaimer

Reference in this report to any specific commercial product, process, or service is to facilitate understanding and does not necessarily imply its endorsement or favoring by the United States Department of Energy.

Acknowledgements

The authors wish to acknowledge financial assistance from the US Department of Energy's National Energy Technical Laboratory (NETL). The project was funded under the Emerging Processing Technology Applications—Gas-to-Liquids Product Line. Programmatic support from Dr Venkat Venkataraman and Dr Daniel Driscoll of the NETL is also gratefully acknowledged. Further, Charles E. Taylor would like to acknowledge the technical assistance of Richard R. Anderson, Edward P. Ladner, Geret Veloski, and Richard P. Noceti.

References

[1] Robertson EP. Options for gas-to-liquids technology in Alaska. INEEL/EXT-99-01023, 1999.
[2] Gladisch H. How Hüels makes acetylene by DC arc. Hydrocarbon Process Petrol Refiner 1962;41:159–64.
[3] Outokumpu Research. HSC Chemistry for Windows. Version 2.03, 1994.
[4] Frenklach M, Wang H. Detailed mechanism and modeling of soot particle formation. In: Bockhorn H, editor. Soot formation in combustion. New York: Springer, 1994. p. 165–92.
[5] Miller R, Peuckert C. Recent developments the production of acetylene from coal by the Hüels arc process. In: Boulos MI, Munz RJ, editors. Proceedings of the Sixth International Symposium on Plasma Chemistry, Montreal, 1983. p. 207–75.
[6] Peuckert C, Müller R. Acetylene from coal by the Hüels plasma process, different operating conditions and their consequences for the process. In: Timmermans CJ, editor. Proceedings of the Seventh International Symposium on Plasma Chemistry, Eindhoven, 1985. p. 274–9.
[7] Holmes JM. Evaluation of DuPont arc process for acetylene and vinyl chloride monomer production. ORNL-TM-2725, 1969.
[8] Lindstedt RP. A simple reaction mechanism for soot formations in non-premixed flames. In: Lee RSL, Whitelaw JH, Wang TS, editors. Proceedings of IVTAM Symposium, Taipei. Springer, 1992. p. 145–56.
[9] Fincke JR, Swank WD, Haggard DC. Transverse injection into a supersonic thermal plasma stream. In: Harry J, editor. Proceedings of the 11th International Symposium on Plasma Chemistry, Loughborough, 1993. p. 168–71.
[10] Detering BA, Donaldson AD, Fincke JR, Kong PC. Fast quench reactor and method. US Patent number 5,749,937, 1998.
[11] Nieuwland JA, Vogt RR. The chemistry of acetylene, ACS Monograph 99. Washington, DC: American Chemical Society, 1945.
[12] Egloff G, Lowry CD, Schaad RF. J Phys Chem 1932;36:1457–520. 1864.
[13] Erdmann H, Koethner P. Z Anorg Chem 1898;18:48–58. 1865.
[14] Heinemann A. US Patent number 1,134,677, 1915.
[15] Winkler F, Hauber H. US Patent number 1,868,127, 1932.
[16] Nieuwland J. Vinyl derivatives of acetylene and method of preparing the same. US Patent number 1,811,959, 1931.
[17] Fields EK, Winzenburg ML, DeMarco DA. Process for preparation of fuel additives from acetylene. US Patent number 4,585,897, 1986.
[18] Wizenburg ML, DeMarco DA. Process for converting a wet acetylene containing stream to aromatics using a zinc-promoted crystalline, borosilicate molecular sieve catalyst composition. US Patent number 4,982,032, 1991.
[19] Timmons RB, He Y, Jang W-L. Zeolite catalyzed conversion of acetylene. US Patent number 5,118,893, 1992.
[20] Givens EN, Plank CJ, Rosinski EJ. Converting low molecular weight olefins over zeolites. US Patent number 3,960,978, 1974.
[21] Reppe W, Wolfe W. US Patent 2,066,076, 1934.
[22] Leutner HW, Stokes CS. Producing acetylene in a plasma jet. Ind Engng Chem 1961;53:341–2.
[23] Anderson JE, Case LK. An analytical approach to plasma torch chemistry. Ind Engng Chem Process Des Dev 1962;1:161–5.
[24] Ibberson VJ, Sen M. Plasma jet reactor design for hydrocarbon processing. Trans Instn Chem Engr 1976;54:265–75.
[25] Plotczyk WW. Effect of quenching temperature of the reaction on the synthesis of acetylene from methane in hydrogen plasma jet. In: Boulos MI, Mouz RJ, editors. Proceedings of the Sixth International Symposium on Plasma Chemistry, Montreal, 1983. p. 300–5.
[26] Kovener GS. Use of an RF plasma for thermal pyrolysis of CH_4 and heavy oils. In: Bovlos MI, Munz RJ, editors. Proceedings of the Sixth International Symposium on Plasma Chemistry, Montreal, 1983. p. 258–63.
[27] Plotczyk WW. Thermodynamic models of acetylene synthesis in an argon plasma jet. In: Timmermans CJ, editors. Proceedings of the Seventh International Symposium on Plasma Chemistry, Eindhoven, 1985. p. 280–5.